J. Micropalaeontology, 43, 475–495, 2024
https://doi.org/10.5194/jm-43-475-2024

Journal of Micropalaeontology
Open Access

Chitinozoan biostratigraphy through the Aeronian–Telychian boundary interval on Anticosti Island, Canada

Carolina Klock[1], André Desrochers[2], Patrick I. McLaughlin[3], Poul Emsbo[4], Tim De Backer[1], Fien M. Jonckheere[1], Cristiana J. P. Esteves[1], and Thijs R. A. Vandenbroucke[1]

[1]Department of Geology, Ghent University, Ghent, Belgium
[2]Department of Earth and Environmental Sciences, University of Ottawa, Ottawa, Ontario K1N 6N5, Canada
[3]Illinois State Geological Survey, University of Illinois, Urbana–Champaign, Illinois 61790-4400, USA
[4]U.S. Geological Survey, Denver Federal Center, Denver, Colorado 80225, USA

Correspondence: Carolina Klock (carolina.klock@ugent.be)

Received: 4 June 2024 – Revised: 24 September 2024 – Accepted: 29 September 2024 – Published: 9 December 2024

Abstract. The well-preserved Llandovery (lower Silurian) succession of Anticosti Island (Quebec, eastern Canada) contains an expanded Aeronian–Telychian boundary interval when compared to other coeval basins. This boundary interval on Anticosti Island also includes two of the most important Llandovery biogeochemical events, the late Aeronian and Valgu events. These two events were previously documented in the Jupiter and Chicotte formations through the study of conodont, graptolite, and brachiopod biostratigraphy and $\delta^{13}C$ chemostratigraphy. Despite these multiple investigations, the exact position of the Aeronian–Telychian stage boundary on Anticosti Island has not been firmly established. Here we locally define and globally correlate chitinozoan biozones to refine the position of this stage boundary. The *Ancyrochitina ramosaspina* biozone, recognized in the Ferrum Member of the Jupiter Formation, correlates with the global *Conochitina alargada* biozone and indicates an Aeronian age. The *Eisenackitina dolioliformis* biozone suggests mostly a Telychian age for the Pavillon Member of the Jupiter Formation and the Chicotte Formation. Three new species are defined, namely *Conochitina asselinae* sp. nov., *Spinachitina glooscapi* sp. nov., and *Ancyrochitina wilsonae* sp. nov. (registration date: 4 December 2024, publication LSID: urn:lsid:zoobank.org:pub:11184506-F273-4D7A-BC28-A1BB4BC8FCD8, asselinae LSID: D282DA9D-6A9C-4B9E-AA6C-9ADC4473E95B, glooscapi LSID: 5801DC12-4EA1-439F-B7C8-FAF7C1B9D2C7, wilsonae LSID: 549EEF2F-7F19-4E6D-9F8E-384594B2FE65). Our new chitinozoan data, combined with previous studies, allow a comparison with the well-studied Baltic succession, confirming that limited unconformities mark the Aeronian–Telychian boundary interval on Anticosti Island, in contrast to the less complete coeval location. Our refined age model for the Aeronian to Telychian succession of Anticosti Island provides a solid baseline to study further Llandovery biochemical events in the aftermath of the Late Ordovician mass extinction.

1 Introduction

1.1 The late Aeronian and Valgu events and Llandovery chitinozoan biostratigraphy

The study of biogeochemical events in the Llandovery remains rudimentary relative to those in the Wenlock and Ludlow series. This focus on the $\delta^{13}C$ and paleontological record of the Wenlock–Ludlow interval can be traced back to the establishment of the "Silurian events" by Jeppsson (1993), i.e., the Ireviken, Mulde, Lau, and Linde events, focused on the temporal space exposed in Gotland, Sweden, and mostly based on conodont work. Much like Gotland, Anticosti Island provides exquisite coastal exposures of almost

structurally unaffected sedimentary rocks. But here, Silurian rocks predating the Wenlock are exposed. However, in the past century, especially in the 1960s, studies on Anticosti mostly focused on the Ordovician–Silurian boundary, assessing hydrocarbon potential in the region (Barnes et al., 1981). Only in the past couple of decades has attention been given to the Llandovery units of the island in the form of stratigraphic and sedimentological studies (e.g., Clayer and Desrochers, 2014; Braun et al., 2021), as well as paleontological investigations (Jin and Copper, 2000; Copper and Jin, 2015). Chitinozoan studies, nevertheless, remained preliminary for the younger units of the island (see Achab, 1981).

Four biogeochemical events are documented in the Llandovery interval, named the early Aeronian, late Aeronian, Valgu, and Manitowoc events, marked by $\delta^{13}C$ excursions in the geological record (e.g., Jeppsson, 1993; Calner, 2008; Munnecke et al., 2010; Cramer et al., 2011; McLaughlin et al., 2019; Melchin et al., 2020). The late Aeronian and Valgu events bracket the Aeronian–Telychian boundary, which is marked by a major unconformity on several paleocontinents (e.g., Baltica in Kaljo et al., 2003, and Munnecke and Männik, 2009; Laurentia in McLaughlin et al., 2019; possibly Gondwana in Caputo and dos Santos, 2020; southern China in Jia-Yu and Johnson, 1996). This boundary interval is well-studied in the eastern Baltic region, where the unconformity is interpreted to span the upper Aeronian *Lituigraptus convolutus* to lower Telychian *Spirograptus turriculatus* graptolite biozones (Loydell et al., 2010), and it highlights the base of the Rumba Formation, characterized by relatively low $\delta^{13}C$ values (Kaljo and Martma, 2000; Munnecke and Männik, 2009). Other disconformities are also recognized in this interval near the top of the Rumba and the FAD (first appearance datum) of *Pterospathodus eopennatus* (Kaljo et al., 2003). The age of the Rumba Formation is debated to be either Aeronian (Kaljo and Martma, 2000) or Telychian (Gouldey et al., 2010; Nestor, 2012) or to straddle the Aeronian–Telychian boundary (Munnecke and Männik, 2009; Walasek et al., 2018).

On Anticosti Island, the Aeronian–Telychian boundary interval is represented by the Jupiter and Chicotte formations. From bottom to top the Jupiter Formation is divided into the Richardson, Cybèle, Ferrum, and Pavillon members. The contact between the two formations is well-exposed in the Jumpers Cliff section on the island. Despite a consensus on the presence of a global unconformity (or unconformities) in the Aeronian–Telychian boundary interval, Braun et al. (2021) interpreted the Jumpers Cliff section of Anticosti Island to be near-conformable, indicating that the magnitude of the unconformity is much shorter on the island than in coeval locations. The $\delta^{13}C$ values for the late Aeronian event, in the Richardson Member of the Jupiter Formation, span from a baseline of 0 to $+1‰$ up to a peak of $+6‰$, while the values for the Valgu event, in the Chicotte Formation, reach up to $+3.5‰$ – these are peak values that have rarely been documented in this interval (Braun et al., 2021).

While several studies have assigned the lower part of the Jupiter Formation (Richardson Member) to the Aeronian stage and the remaining higher members of the Jupiter Formation (Cybèle, Ferrum and Pavillon members) and the Chicotte Formation to the Telychian stage, the precise position of the Aeronian–Telychian boundary within the Anticosti succession is uncertain. Zhang and Barnes (2002) and Munnecke and Männik (2009) interpreted the Pavillon Member to be in the *Distomodus staurognathoides* conodont biozone, which could be late Aeronian or Te1 (stage slices sensu Melchin et al., 2020) in age. Munnecke and Männik (2009) studied the conodonts of the Chicotte Formation as well and concluded that the unit is already in the *Pterospathodus eopennatus* biozone, indicating a likely Te2 age. Additional reasoning in the literature for the interpretation of a Telychian age for the Cybèle Member and younger units of the island is that the upper Aeronian *Stimulograptus sedgwickii* graptolite biozone was clearly identified in the Richardson Member (Riva and Petryk, 1981), underlying the Cybèle Member. The authors interpreted the finding of the index fossil of this biozone to mark the top of the Aeronian on Anticosti. It is noteworthy that neither *sedgwickii* nor other graptolite species have been found in the Cybèle and Ferrum members, so Jin and Copper (2000) attempted to clarify the relative dating of the units using brachiopod biozones. The Ferrum Member is assigned to the *Strickandia planirostrata* biozone, as is the underlying Cybèle Member, but the most useful pentamerids for biostratigraphy in this interval in Baltica and Avalonia (i.e., *Stricklandia lens*) are not identified on Anticosti (Jin and Copper, 2000, p. 21). Authors have interpreted the age of the *Strickandia planirostrata* biozone as early Telychian as they found it above the *sedgwickii* graptolite levels of the Richardson Member. However, the strata above the Richardson Member could also still be part of the upper *sedgwickii* graptolite chronozone given the absence of graptolite data in the Cybèle and Ferrum members. Altogether, conodont, brachiopod, and graptolite biostratigraphic data have not provided an entirely convincing age for the Ferrum Member.

The *Pentameroides subrectus–Costistriscklandia gaspeensis* brachiopod biozone was identified in the Pavillon Member of the Jupiter Formation and in the Chicotte Formation. The appearance of *Pentameroides subrectus* associated with *Costistricklandia gaspeensis* is time-equivalent to the *Monoclimacis griestoniensis* graptolite biozone (e.g., Cocks and Worsley, 1993; Jin, 2002). Thus, the Pavillon Member and the lower Chicotte Formation have been interpreted to have a Telychian age.

Given that the graptolite record is absent in most units of Anticosti Island and that the conodont yield is usually low in the Silurian, with long-ranging global biozones, chitinozoans are a promising fossil group to refine the relative dating of the members of the Jupiter Formation. A caveat to using lower Llandovery chitinozoan biozones is that they are still a work in progress, despite the seminal review by Verniers

et al. (1995), who formally defined a "global" chitinozoan biozonation for the Silurian System. Most of the defined biozones for the lower to mid-Llandovery are based on data from the Baltic Basin (e.g., Nestor, 1980a, 1980b, 1990, 1994), except for the zone based on *Conochitina alargada*, a species defined in the Spanish Cantabrian Mountains by Cramer (1967). Nestor (2012) reviewed the biostratigraphy of the Baltic Basin and, specifically in the Llandovery, named an interzone – due to poor chitinozoan content – from the middle of Rh1 to early Rh2 and a barren interval between Ae3 and almost the end of Te1, which confirmed the need to reassess those intervals in different sedimentary basins (for a definition of time slices, see Cramer et al., 2011). On Anticosti Island, chitinozoan biostratigraphic studies have hitherto been primarily focused on the Ordovician–Silurian boundary interval. The Ellis Bay and Becscie formations (Hirnantian to Rhuddanian) have received the most attention from chitinozoan biostratigraphers (Soufiane and Achab, 2000; Achab et al., 2011, 2013). These studies have also provided some information about the chitinozoan biozonation of the Merrimack and Gun River formations, while the chitinozoan data on the younger units (i.e., Menier and Jupiter formations) remain limited to preliminary reports in Achab (1981).

The nearly continuous lithological record of Anticosti during the Aeronian–Telychian boundary interval, together with the established $\delta^{13}C$ record that pinpoints the Valgu event, makes this interval a prime target to reinvestigate mid-Llandovery chitinozoan biostratigraphy. Thus, this study aims to add to this body of research by presenting a new chitinozoan biostratigraphy across the Aeronian–Telychian boundary by targeting the Ferrum and Pavillon members of the Jupiter Formation as well as the Chicotte Formation at the well-exposed Jumpers Section on Anticosti Island.

1.2 Geological setting

Anticosti Island is in northeastern Quebec, Canada, a portion of St. Lawrence carbonate platform during the time of deposition (Fig. 1). During the early Silurian, it was part of the paleocontinent Laurentia, located at about 20°S paleolatitude (Merdith et al., 2021), with deposition occurring within a relatively shallow tropical marine environment. The crystalline basement of the Anticosti Basin is overlain by 2 km of Ordovician strata and 0.5 km of Silurian strata (McLaughlin et al., 2016; Desrochers et al., 2023). Deposition was storm-dominated and occurred along a southwest-dipping ramp, with mixed carbonate–siliciclastic facies in the east part of the island and carbonate facies in the middle and western part (e.g., Sami and Desrochers, 1992; Long, 2007; Desrochers et al., 2010). The remarkably thick carbonate-dominated succession is exceptionally well-preserved, never having been deeply buried or structurally deformed, with the exception of minor folding, faults, and fractures or jointing related to far-field strain from subsequent orogenesis (Barnes, 1988; Desrochers, 2006; Bordet et al., 2010; Pinet et al., 2012, 2015). Prominent disconformities are present on the eastern portion of Anticosti, such as incised valley systems; however, they are not traceable into the central and western parts of the island (Desrochers et al., 2010; Zimmt et al., 2024).

The Silurian stratigraphy of Anticosti Island is divided into six formations, including the Becscie, Merrimack, Gun River, Menier, Jupiter, and Chicotte formations that cover, from bottom to top, 500 m of sequence (Copper and Long, 1990; Copper and Jin, 2012, 2014, 2015). This study focuses on the upper Jupiter (Ferrum and Pavillon members) and Chicotte formations (Fig. 2a, b). The Ferrum Member is composed of bioclastic wackestone to packstone, interbedded with crinoid-rich calcarenite and calcareous shale, whereas the Pavillon Member is finer-grained and dominated by argillaceous lime mudstone and calcareous shale (Clayer and Desrochers, 2014). The Chicotte Formation is composed primarily of coarse crinoidal grainstones (Clayer and Desrochers, 2014; Braun et al., 2021).

The samples for this study were collected from the Jumpers Cliff section (see zoom in Fig. 1; coordinates 49.381410953673495, −63.53606778415303), located in the southern part of the island, 4 km east of the Southwest Point lighthouse. In the Jumpers Cliff section, the thickness of the Ferrum Member is 3 m, the Pavillon Member is about 5 m, and the Chicotte Formation is less than 6 m (Clayer and Desroches, 2014). The Ferrum and Pavillon members of the Jupiter Formation in the Jumpers Cliff section were deposited in an inner ramp to mid-ramp, in a seemingly continuous record, while the Chicotte Formation was deposited in a more distal mid-ramp, and its contact with the underlying Pavillon Member likely marks a disconformity (Clayer and Desrochers, 2014).

2 Material and methods

2.1 Samples

A total of 25 samples were collected in parallel with those for the study published by Braun et al. (2021) at the well-studied Jumpers Cliff section (see Clayer and Desrochers, 2014). The section is a coastal rock exposure 14 m high. The base of the outcrop begins in the upper portion of the Jupiter Formation and the top is in the lower portion of the Chicotte Formation. Samples were generally collected at 0.5 m spacing, with 6 taken from the Ferrum Member, 11 from the Pavillon Member, and 8 from the Chicotte Formation.

2.2 Analytical techniques

Samples from Jumpers Cliff were processed for chitinozoan study using traditional palynological techniques. In the lab, samples were first washed to remove superficial impurities and were broken into smaller pieces. Subsamples separated for digestion ranged from about 160 to 230 g in limestones and from about 50 to 120 g in shales. The exception was the

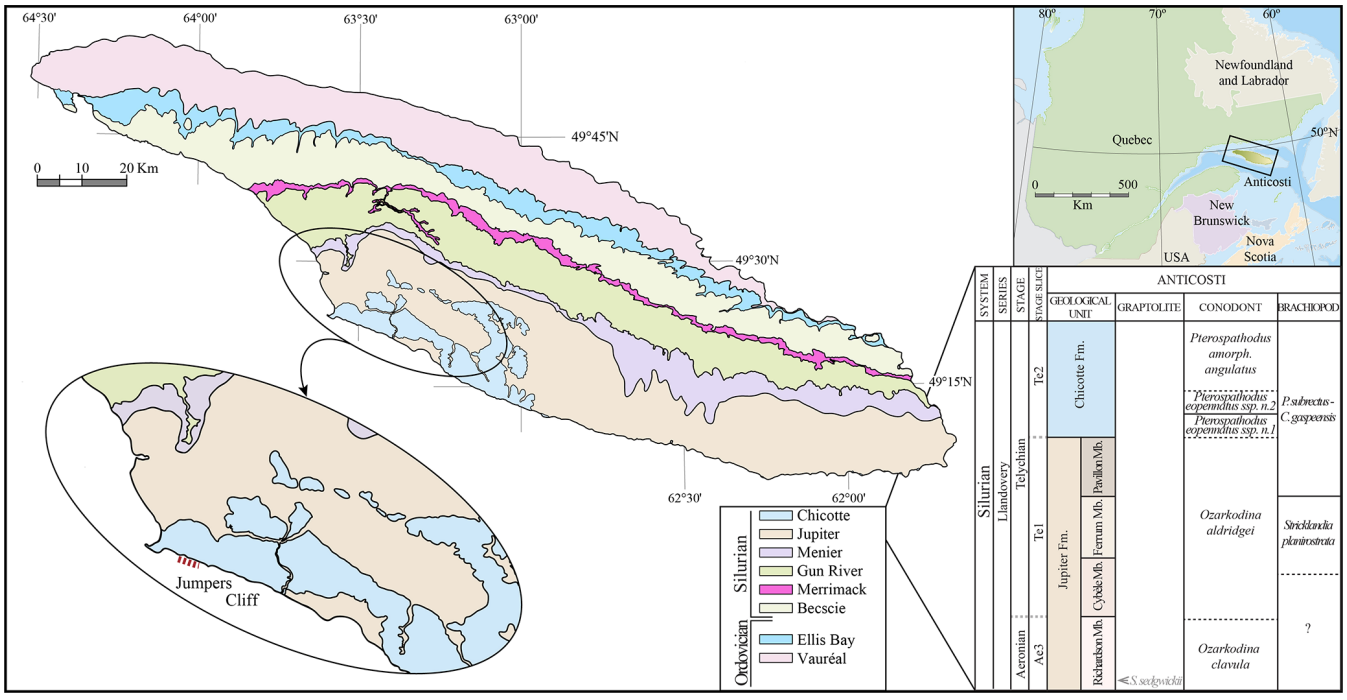

Figure 1. Location of Anticosti and a geological map of the island. The stratigraphic column shows the members of the Jupiter Formation and the Chicotte Formation, with the local graptolite, conodont, and brachiopod biozones, as well as the previous interpretation of the Aeronian–Telychian boundary on the island (modified from Melchin et al., 2020, and Braun et al., 2021).

Figure 2. **(a)** Contact between the Ferrum (bottom unit, distinguished in this photo by a recessive pattern on the cliff) and Pavillon (middle unit, marl-dominated, marked in this photo by its crumbly aspect) members of the Jupiter Formation. The Chicotte Formation is also exposed at the very top of the picture, with a beige–yellowish color. **(b)** Exposure of the Chicotte Formation on the cliff, as well as fallen blocks. The original position of the blocks on the cliff could be easily reconstructed in the field.

shale sample JM-24, from the Chicotte Formation, a unit that otherwise was unproductive for chitinozoans in the encrinite samples – its predominant lithology. Digestion of the disaggregated samples using hydrochloric and hydrofluoric acids followed the protocols of Paris (1981) and Sutherland (1994). After digestion of the rock matrix, a Zeiss Discovery V20 stereomicroscope was used to hand-pick the organic fraction larger than 53 µm. A total of 300 chitinozoan specimens were picked in residues where the amount was available, and otherwise the entire residue was picked. The specimens were placed onto 12 mm aluminum stubs, gold-coated, and systematically photographed and identified using a TESCAN scanning electron microscope TIMA3-X GMU. The stubs containing the photographed specimens and the paly-

nomorph residues are stored in the collections of the Department of Geology, Ghent University, Belgium.

2.3 Measurements of chitinozoan features

A series of measurements were executed on the chitinozoans following specifications in Paris et al. (1999) and using the Fiji image processing package. Diameter measurements are given in raw numbers, without corrections applied. Table 1 specifies the measurements conducted. In this paper, $\overline{x}$ is used to refer to the "average".

3 Results

Most samples from the Jumpers Cliff section produced well-preserved and zonally diagnostic chitinozoans. Chitinozoan abundances were highest in the Pavillon Member, with 5 out of 11 samples yielding fewer than 300 chitinozoans for 46 to 120 g of sample (JM-07, JM-08, JM-10, JM-15, and JM-17). The Ferrum Member samples were less productive, with four out of six samples producing fewer than 300 chitinozoans for 166 to 231 g of sample (JM-01, JM-02, JM-04, and JM-05). The yield was the lowest in the Chicotte Formation, where most samples (where the lithology was encrinite) were barren of chitinozoans, with the exception being sample JM-24, collected from a shale bed. Although not studied systematically, residues also produced many well-preserved acritarchs, scolecodonts, melanosclerites, and fragments of graptolites (here listed in order of abundance).

The chitinozoans are well-preserved and this did not vary stratigraphically. A total of 22 chitinozoan taxa were identified, with 12 classified as known species and three new species discovered (Table 2 and Figs. 3–6). Where identification was limited to the generic level, this was due to the lack of definitive characters (e.g., *Conochitina* spp., *Cyathochitina* spp., and *Bursachitina* spp.) or due to the poor preservation of the ornamentation (e.g., *Ancyrochitina* spp. and *Angochitina* spp.), and open nomenclature followed the guidelines of Bengtson (1988).

Systematic notes on selected taxa are presented below. The organic residues, rocks, and stubs with counted specimens are stored in the collections of the Department of Geology at Ghent University (under the same numbers as used for sample numbers in this paper). Described holotypes and paratypes have been mounted on permanent slides and transferred to the museum collections of the Royal Belgian Institute of Natural Sciences in Brussels (RBINS) for permanent curation (RBINS collection numbers b9970 to b9985).

Systematic descriptions

Incertae sedis group Chitinozoa Eisenack, 1931

Order Prosomatifera Eisenack, 1972

Family Conochitinidae Eisenack, 1931 emend. Paris, 1981

Subfamily Conochitininae Paris, 1981

Genus *Conochitina* Taugourdeau, 1966 emend. Paris, Grahn, Nestor and Lakova 1999

Species *Conochitina asselinae* sp. nov.

Figure 3k–p

Measurements (20 specimens)
Total length: 192 to 452 µm, $\overline{x} = 280$ µm
Chamber diameter: 72 to 106 µm, $\overline{x} = 89$ µm
Neck diameter: 50 to 79 µm, $\overline{x} = 67$ µm
Wall thickness: 1.5 to 3.9 µm, $\overline{x} = 2.5$ µm
Mucron length: 0 to 6.2 µm, $\overline{x} = 2.9$ µm
Mucron width: 12 to 25 µm, $\overline{x} = 18$ µm
Material: 96 specimens (incl. Fig. 3k = RBINS b9981; Fig. 3l = RBINS b9982; Fig. 3m = RBINS b9983; Fig. 3n = RBINS b9984; Fig. 3p = RBINS b9985)
Holotype: Figure 3o (RBINS collection number b9980)
Holotype dimensions: total length = 267 µm; chamber diameter = 91 µm; neck diameter = 73 µm; wall thickness = 3.0 µm; mucron size = 2.5 µm; mucron width = 17 µm
Type stratum: Chicotte Formation (sample JM-24)
Derivatio nominis: species named after Esther Asselin, who made important contributions to the micropaleontological studies on Anticosti Island

Description. R ranges between 2.4 and 4.9, usually being around 3.6. The shape of the chamber is cylindro-conical, with the flexure in the prosome region clearly marking the division between the neck and chamber; the vesicle has, in most cases, concave flanks. More rarely, this restriction below the neck is absent and the flanks are straight. The neck is cylindrical when it is longer and conical when it is shorter. The lips are thinly and regularly serrated. The walls have moderate thickness, with an average of 2.5 µm. The chamber is fully and coarsely ornamented by a thick granular to rugous texture, inherent to the walls. This texture stops at the flexure, leaving the neck unornamented. The base presents a well-marked mucron that is highly ornamented, with a clearly unornamented pit.

The ornamentation of the vesicle is intrinsic to the external surface of the upper layer of the wall (Fig. 3p1) and is not elevated, so "rugous" strikes us as the most accurate descriptive term.

Remarks. Conochitina asselinae differs from existing *Conochitina* species due to its full to nearly full coverage of the chamber by coarse granules. Given that the ornamentation does not characterize spines (i.e., length twice the width and total size exceeds 2 µm; Paris et al., 1999), including it in the subfamily *Conochitininae* is preferred over *Belonechitininae*.

Occurrence. Present in the Chicotte Formation.

Conochitina edjelensis – Conochitina elongata group (Taugourdeau, 1963)

Figure 3. A – JM-11, B – JM-12: *Calpichitina densa* Eisenack (1962), 100 µm scale bar. C – JM-17, D – JM-17, E – JM17, F – JM-17: *Eisenackitina dolioliformis* Umnova (1976), 100 µm scale bar. G – JM-02, H – JM-05, I – JM-05, J – JM-05: *Euconochitina electa* Nestor (1980a), 100 µm scale bar. O – JM-24, holotype of *Conochitina asselinae* sp. nov., 100 µm scale bar. K – JM-24, L – JM-24, M – JM-24, N – JM-24, P – JM-24: variety range of *Conochitina asselinae* sp. nov., 100 µm scale bar. P1: zoom of mucron and inherent wall texture of *Conochitina asselinae* sp. *nov.*, 50 µm scale bar.

Table 1. List of chitinozoan features and the description of measurements. For a definition of chitinozoan features, see Paris et al. (1999). The list also includes codes used (i.e., P and R) and their numeric meaning. The symbol $\overline{x}$ was used in its conventional statistical meaning of average.

Features or codes	Descriptions
Total length	Distance from lip to apex.
Neck length	Distance from lip to flexure (or total length − chamber length).
Chamber length	Distance from flexure to apex (or total length − neck length).
Chamber diameter	If the base is flat, measurement of the base. If the base is concave or convex, measurement of the maximum diameter of the chamber.
Neck diameter	Measurement of the maximum diameter of the neck.
P	Neck length / chamber length.
R	Total length / $\overline{x}$ chamber diameter.
Wall thickness	Measured on the flanks. Sections on the middle part of the body preferred, as the thickness normally varies from top to bottom. However, in cases where the specimen was only locally broken on the top or bottom, the measurements were performed there. Classified as thin when < 1.5 µm, moderate when between 1.5 and 3.0 µm, and thick when > 3.5 µm.
Mucron length	Height of the mucron.
Apical structure width	Diameter of the apical structure.
Spine size	Extension of the largest spine.
Process size	Extension of the largest process.
Number of processes	Normally inferred due to either the limited lateral view of a single side of the specimen or, in this case, the observed number having been multiplied by 2 to replicate the hidden side; often additionally inferred due to the destruction and/or poor preservation of certain processes.

Figure 4a–e

Measurements (50 specimens)
Total length: 137 to 465 µm, $\overline{x} = 235$ µm
Chamber diameter: 60 to 116 µm, $\overline{x} = 84$ µm
Material: 692 specimens

Remarks. *Conochitina edjelensis elongata* was originally defined as a subspecies of *Conochitina edjelensis* by Taugourdeau (1963), largely based on its total length. The total length of the holotype of *Conochitina edjelensis* is 150 µmm, whereas the holotype of *Conochitina edjelensis elongata* is 205 µm. The 50 specimens measured in this study show a gradient increase in size (Fig. 7), starting from what would be considered *Conochitina edjelensis* and ending over twice as large as the original holotype of *Conochitina edjelensis elongata*. Given that variation in size happens along a continuous trend, we cannot separate the assemblage into two groups based on the total lengths of the specimens. All things considered, we show the total assemblage as a group combining *Conochitina edjelensis* and *Conochitina edjelensis elongata* with an extreme range of total length.

Occurrence. Present in both the Ferrum Member and the Pavillon Member of the Jupiter Formation.

Subfamily Spinachitininae Paris, 1981

Genus *Spinachitina* Schallreuter, 1963

Spinachitina glooscapi sp. nov.

Figure 5g–j

Measurements (15 specimens)
Total length: 330 and 536 µm
Minimum length (specimens were latitudinally broken) = 208 to 694 µm, $\overline{x} = 394$ µm
Chamber diameter: 60 to 113 µm, $\overline{x} = 87$ µm
Neck diameter: 38 to 64 µm, $\overline{x} = 51$ µm
Wall thickness: 1.4 to 3.9 µm, $\overline{x} = 2.3$ µm
Process size: 2 to 9 µm, $\overline{x} = 5$ µm
Number of processes: 20 to 36, $\overline{x} = 26$
Material: 18 specimens (incl. Fig. 5g = RBINS b9971; Fig. 5h = RBINS b9972; Fig. 5j = RBINS b9973)
Holotype: Figure 5i (RBINS collection number b9970)
Holotype dimensions: total length = 597 µm; chamber diameter = 94 µm; neck diameter = 54 µm; wall thickness = 2.1 µm; process size = 5 µm; number of processes = 28
Type stratum: Pavillon Member, Jupiter Formation, sample JM-12

https://doi.org/10.5194/jm-43-475-2024

Table 2. Numerical results of the study of 25 samples of the mid-Llandovery interval from Anticosti Island.

			Chitinozoan species																						
Sample code	Geological unit	Sample size (g)	*Angochitina* sp. A	*Conochitina edjelensis–Conochitina elongata* group	*Conochitina gunriveris*	*Conochitina malleus*	*Conochitina praeproboscifera*	*Euconochitina electa*	*Ancyrochitina ramosaspina*	*Angochitina* sp. B	*Conochitina leptosoma*	*Cyathochitina campanulaeformis*	*Cyathochitina caputoi*	*Eisenackitina dolioliformis*	*Conochitina emmastensis*	*Spinachitina glooscapi* sp. nov.	*Calpichitina densa*	*Conochitina asselinae* sp. nov.	*Ancyrochitina wilsonae* sp. nov.	*Conochitina* spp.	*Ancyrochitina* spp.	*Angochitina* spp.	*Cyathochitina* spp.	*Bursachitina* spp.	Chitinozoan indet.	Total
JM-27		203.9																								0
JM-24		51.7			19	25								20				96	78	16	32			22	48	356
JM-23		221.8																								0
JM-22	Chicotte	195.7																								0
JM-21	Formation	199.4																								0
JM-20		181.9																								0
JM-19		172.8																								0
JM-18		203.3																								0
JM-17		46.2		2		1	1				1	1		64	14					2	56		1		11	153
JM-16		52.1		87	7	10	22					1		1	82					36	62	1			39	348
JM-15		56.8		45	6	28	2							2	2					18	88	1			25	217
JM-14	Pavillon	51.0		16	8	84	7								1					40	121	3			26	306
JM-13	Member –	50.3		77	2	2	2				4	3	30		2	6				39	127		14		21	329
JM-12	Jupiter	49.4		58	6	4	1				18	5	5	1	5	10	4			27	184		10		25	363
JM-11	Formation	51.4		126	8	4	4					8	40		10		2			54	39	3	23	2	18	341
JM-10		46.6		43	2	20	11				1	7	81		1		3			26	63		8		32	297
JM-09		53.1		114		1							23	2		2				27	90		15	1	25	300
JM-08		60.5		2		1	1						6	1	24					16	37		10	2	7	109
JM-07		121.2	55	25	41	15	12						9	1						46	34	6			19	261
JM-06		166.7	1	33	13	2		18	88											22	188	2			19	386
JM-05	Ferrum	206.0	1	36	17	1	3	25	23			17	18							14	56	3	12		13	239
JM-04	Member –	200.9	3	10	20	3		16	1	5		86	108							7	2	2	99		9	374
JM-03	Jupiter	202.4	5	14	15	1		31	8	2		35	27							16	7	3	41		27	232
JM-02	Formation	231.0	1	3	8			3	1	1	1									1	3				13	35
JM-01		202.0	1	1	10	9	2	2												9	9	1			37	81

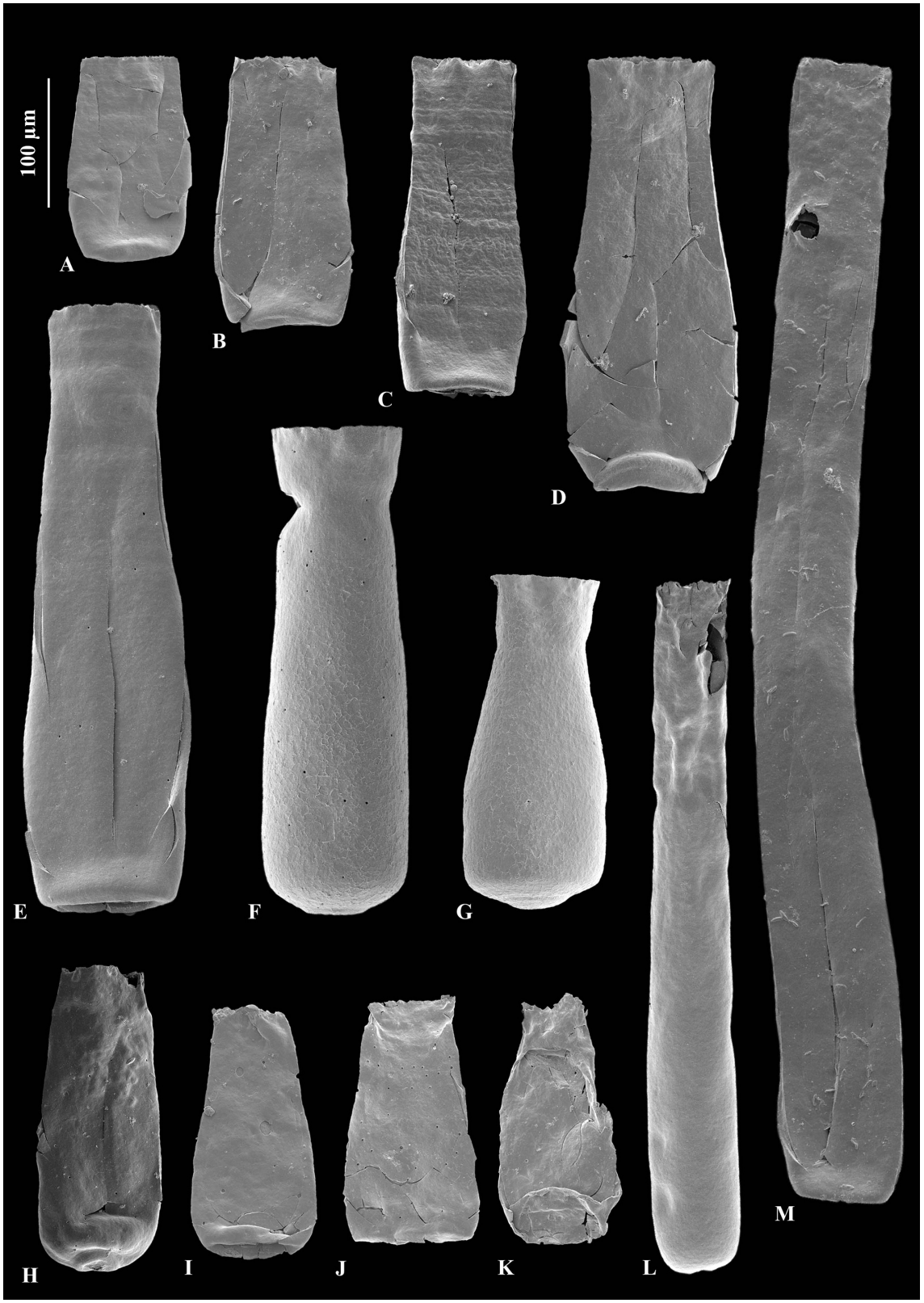

Figure 4. A – JM-09, B – JM-12, C – JM-08, D – JM-11, E– JM-11: *Conochitina edjelensis–Conochitina elongata* group illustrating the large range in sizes of specimens in the group. F – JM-15, G – JM-15, H – JM-10: *Conochitina emmastensis* Nestor (1982). I – JM-24, J – JM-07, K – JM-01: *Conochitina gunriveris* Soufiane and Achab (2000). L – JM-02, M – JM-12: *Conochitina leptosoma* Laufeld (1974).

Derivatio nominis: species named after Glooscap, a legendary being of Canadian Aboriginal origin (Mi'kmaq, Maliseet, Passamaquoddy, Penobscot, and Abenaki), great in size and power, who is told, amongst other things, to have made the world habitable (Canadian Museum of History, 2023)

Description. R is, on average, 5.7, but it ranges from 3.6 to 8.0. The chamber shape is conical, with straight flanks – less commonly, they can present a discreet flexure at the bottom of the neck. The margins make an angle close to 90°. The aperture flares out towards the lips, which have a regular and straight margin. The wall has a moderate thickness, averaging 2.3 µm. The neck and most of the chamber are unornamented, except for the basal part of the specimens, which can be granular. A large number of processes can be observed, and they are short (< 10 µm). It is not unusual for these processes to be totally or partially removed during the taphonomic process. No other apical structures are present.

Remarks. Spinachitina glooscapi sp. nov. differs from *Spinachitina harringtoni* in size and number of processes. *S. harringtoni* has a maximum vesicle size of 543 µm (Grahn et al., 2000), while the new species described here reaches up to 694 µm. *S. harringtoni* also has fewer processes: 10 to 12 compared to the 20 to 36 marginal spines of *S. glooscapi* sp. nov. Therefore, *S. glooscapi* sp. nov. is normally larger than *S. harringtoni* and presents at least twice as many spines at the base of the vesicle. It is possible that the two species are somewhat related.

Occurrence. Locally within the Pavillon Member of the Jupiter Formation.

Family Lagenochitinidae Eisenack, 1931

Subfamily Angochitininae Paris, 1981

Genus *Angochitina* Eisenack, 1931

Species *Angochitina* sp. A

Figure 6d–f

Measurements (20 specimens)
Total length: 130 to 190 µm, $\overline{x} = 170$ µm
Chamber diameter: 73 to 100 µm, $\overline{x} = 88$ µm
Neck diameter: 29 to 48 µm, $\overline{x} = 41$ µm
Wall thickness: 0.7 to 1.9 µm, $\overline{x} = 1.1$ µm
Spine size: 3 to 9 µm, $\overline{x} = 5$ µm
Material: 67 specimens

Description. P is around 0.9 but can also decrease and increase to 0.6 and 1.4, respectively. The flexure can be very prominent, which is possibly the most distinctive feature of this species, and shoulders are not apparent. The chamber shape is ovoid with a rounded base both in 3D and flattened specimens. The neck has a flaring shape towards the aperture, and the lip ridge, when preserved, is coarsely serrated. The spines can vary in size within the same specimen – the longest spines of individuals are, on average, 5.4 µm long. The spines can assume a mesh-like structure around the aperture. Density of ornamentation is also varied, but the spines are distributed in discrete parallel lines. Spines are frequently single- or double-rooted and unified at the tip. Rarely, spines can have three or more roots. No apical structures are observed.

Remarks. For *Angochitina* sp. A, the most distinctive feature is its prominent flexure. There are some similarities to *Angochitina longicollis*, such as the parallel alignment of rows of spines and an ovoid chamber (see fig. 19B of Laufeld, 1974). However, the neck of *Angochitina* sp. A is too short proportionally to the chamber in comparison with *Ancyrochitina longicollis* (Eisenack, 1959). The shape and proportions are comparable to *Angochitina valentinii*; however, due to the less accentuated flexure of *valentinii*, limited imaging in the bibliography, and the lack of a detailed description on the size, the arrangement and shape of its spines (Cramer, 1964) hamper a detailed comparison.

Occurrence. Present in the Ferrum Member of the Jupiter Formation; also occurs, punctually, in the Pavillon Member of the Jupiter Formation.

Species *Angochitina* sp. B

Figure 6g–h

Measurements (7 specimens)
Total length: 171 to 200 µm, $\overline{x} = 185$ µm
Chamber diameter: 86 to 65 µm, $\overline{x} = 75$ µm
Neck diameter: 28 to 42 µm, $\overline{x} = 33$ µm
Wall thickness: 0.9 to 1.3 µm, $\overline{x} = 1.1$ µm
Spine size: 2.9 to 5.9 µm, $\overline{x} = 4.2$ µm
Material: 8 specimens

Description. P average is 1.5, and the range is from 1.3 to 1.8, meaning that the neck is always longer than the chamber. The flexure is conspicuous, shoulders are not present, and the chamber shape is conical. The neck flares towards the aperture, especially at the lip ridge, which is serrated. The size of the spines (average of 4.2 µm) and coverage of the body are consistent within specimens. The distribution of the spines in incipient parallel lines is not uncommon. Spines are frequently double-rooted and unified at the tip. No apical structures are observed.

Remarks. Angochitina sp. B is different from *Angochitina* sp. A in its larger neck relative to the chamber. It is similar to the short morphotype of *Angochitina macclurei* (Paris and Al-Hajri, 1995) in general shape (i.e., neck versus chamber proportions, spine coverage of the body); however, *Angochitina* sp. B is smaller and has a conical – rather than spherical or oval – chamber. *Angochitina* sp. B is also similar to *Sphaerochitina palestinaense* (Grahn et al., 2005). However, all their common features are more exaggerated in *palestinaense*, such as the proportionally longer neck than the chamber and the flaring collarette. Like *macclurei*, *palestinaense* has a spherical to oval chamber, contrasting with the clearly conical chamber of *Angochitina* sp. B.

Figure 5. A – JM-24, B – JM-10, C – JM-14: *Conochitina malleus* Van Grootel (*nomen nudum*) in Nestor (2012). D – JM-16, E – JM-12, F – JM-16: *Conochitina praeproboscifera* Nestor (1994). G – JM-12: holotype of *Spinachitina glooscapi* sp. nov. H – JM-13, I – JM-12, J – JM-09: *Spinachitina glooscapi* sp. nov. K – JM-04, L – JM-04, M – JM-04: *Cyathochitina campanulaeformis* Eisenack (1931).

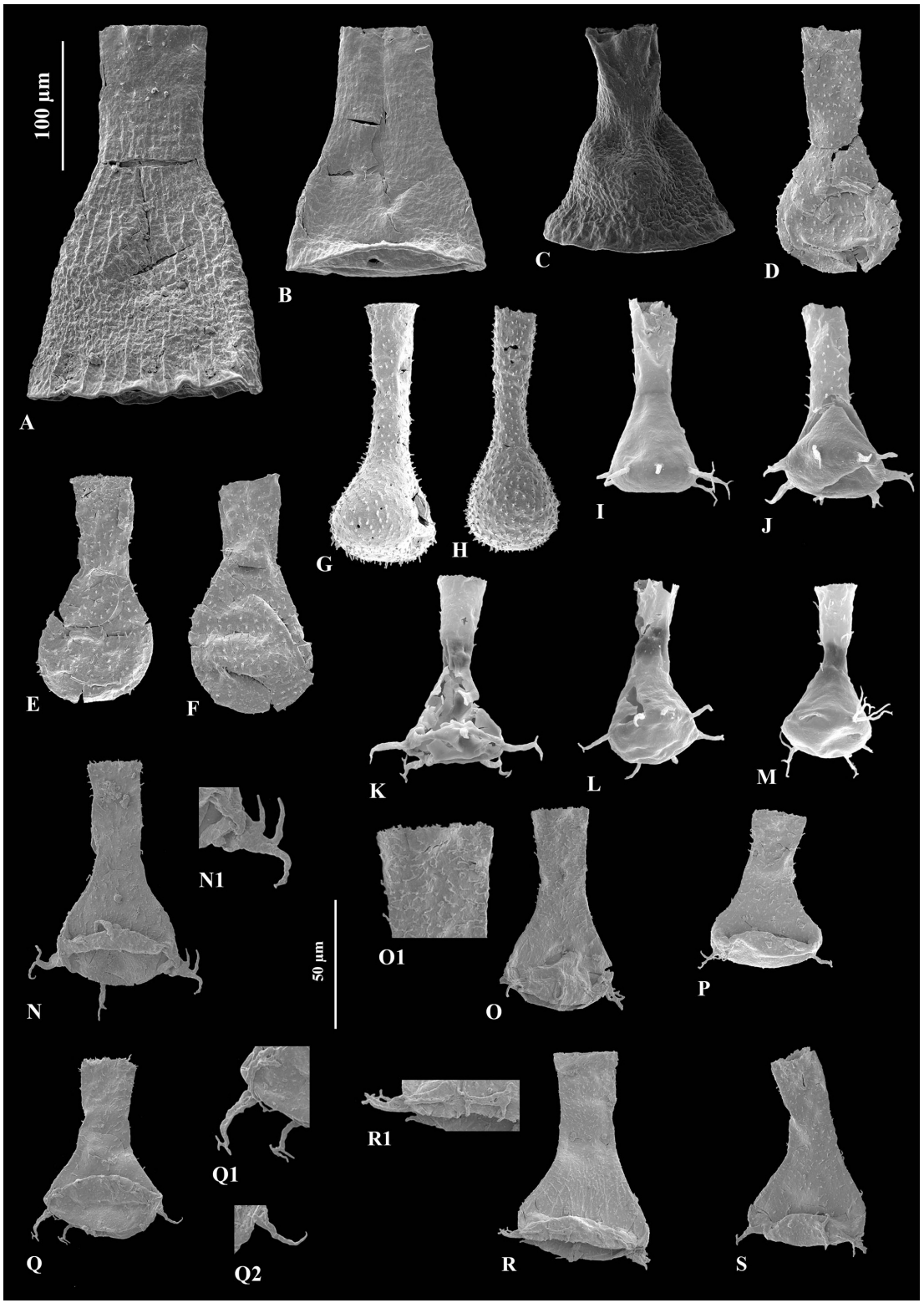

Figure 6. A – JM-10, B – JM-12, C – JM-10: *Cyathochitina caputoi* Da Costa (1971), 100 µm scale bar. D – JM-07, E – JM-07, F – JM-07: *Angochitina* sp. A, 100 µm scale bar. G – JM-03, H – JM-02: *Angochitina* sp. B, 100 µm scale bar. I – JM-05, J – JM-06, K – JM-05, L – JM-06: *Ancyrochitina ramosaspina* Nestor (1994), 100 µm scale bar. M – JM-05: possibly deformed specimens of *Ancyrochitina ramosaspina* based on one aberrantly branched basal process, 100 µm scale bar. N – JM-24: holotype of *Ancyrochitina wilsonae* sp. nov., 100 µm scale bar. O – JM-24, P– JM-24, Q – JM-24, R – JM-24, S – JM24: variety range of *Ancyrochitina wilsonae* sp. nov., 100 µm scale bar. **(N1, O1, Q1, Q2, R1)** Zooms of the diagnostic features of *Ancyrochitina wilsonae* sp. nov., 50 µm scale bar.

Occurrence. Appears in the Ferrum Member of the Jupiter Formation.

Subfamily Ancyrochitininae Paris, 1981

Genus *Ancyrochitina* Eisenack, 1955

Species *Ancyrochitina wilsonae* sp. nov.

Figure 6n–s

Measurements (20 specimens)
Total length: 109 to 178 µm, $\overline{x} = 137$ µm
Chamber diameter: 72 to 98 µm, $\overline{x} = 87$ µm
Neck diameter: 34 to 42 µm, $\overline{x} = 38$ µm
Wall thickness: 0.5 to 1.5 µm, $\overline{x} = 0.9$ µm
Spine size: 2 to 14 µm, $\overline{x} = 6$ µm
Processes size: 14 to 34 µm, $\overline{x} = 23$ µm
Number of processes: 4 to 10, $\overline{x} = 6$
Material: 78 specimens (incl. Fig. 6o = RBINS b9975; Fig. 6p = RBINS b9976; Fig. 6q = RBINS b9977; Fig. 6r = RBINS b9978; Fig. 6s = RBINS b9979)
Holotype: Figure 6n–n1 (RBINS collection number b9974)
Holotype dimensions: total length = 178 µm; chamber diameter = 98 µm; neck diameter = 39 µm; wall thickness = 1.0 µm; spine size = 14 µm; process size = 34 µm; number of processes = 4 (well-developed, plus 1 or 2 – if mirrored – underdeveloped)
Type stratum: Chicotte Formation, sample JM-24
Derivatio nominis: species named after Alice Wilson, Canada's first female geologist, also a paleontologist, who made significant scientific contributions with regards to the rocks and fossils of the Ottawa region

Description. P ranges between 0.6 and 1.7, with an average of 1.2. The flexure is moderate to smooth, and shoulders are absent. The shape of the chamber is conical, transitioning to a conical neck, discretely flaring towards the lip. The lip, when it is well-preserved, is serrated and normally thin and regular, but the serration can also be coarse and irregular. The walls are thin and ornamented with single-rooted spines of 2 to 14 µm. Rarely, a vein-like, vertical structure is observed on the walls of the chamber (Fig. 6r). Spines can be situated on top of these structures but do not seem to be aligned with them. The number of basal processes can range from 4 to 10, being 14 to 34 µm long, and they are often amalgamated together at the base and/or branch out latitudinally into two or three towards the tip.

Remarks. Ancyrochitina wilsonae sp. nov. is a highly ornamented species, with spines on both the walls of the neck and chamber, as well as complex processes. It mainly differs from *Ancyrochitina udayanensis* (Paris and Al-Hajri, 1995) as it is larger than the characteristically small-sized (78 to 104 µm, $\overline{x} = 90$ µm) vesicles of *Ancyrochitina udayanensis*. The number of processes in the new species described here is also inconsistent with those described in *Ancyrochitina udayanensis*: *Ancyrochitina wilsonae* sp. nov. averages around four to six processes, in contrast with the apparently consistent eight processes of *Ancyrochitina udayanensis*. The neck of *Ancyrochitina wilsonae* sp. nov. is also usually longer than the chamber, opposingly to the contrasting species. The new species presents a coincident total length, number of processes, and shape of processes with *Ancyrochitina ancyrea* (Eisenack, 1931). However, Eisenack (1931) specifically states that the spines of *ancyrea* are absent on the lower half of the neck and on the chamber, which is not the case for *Ancyrochitina wilsonae* sp. nov.

Occurrence. Occurs in the Chicotte Formation.

4 Discussion

4.1 Chitinozoan biostratigraphy

The chitinozoans recovered in the Jumpers Cliff samples are sufficiently well-preserved and diverse to support a robust biostratigraphic interpretation. In general, the taxa represent a characteristic lower Silurian assemblage (sensu Verniers et al., 1995; Nestor, 2012), with some newly defined species (Figs. 3, 5, and 6). Two biozones are recognized. The *Ancyrochitina ramosaspina* biozone was locally established on Anticosti Island by Soufiane and Achab (2000), and we follow their definition (i.e., the biozone corresponds to the total range of the index species). The base of the *Eisenackitina dolioliformis* biozone is defined by the lowest (local) occurrence (LO) of the index taxon (Verniers et al., 1995). The biozones were correlated with the global Silurian chitinozoan zonation of Verniers et al. (1995).

4.1.1 *Ancyrochitina ramosaspina* biozone

The *Ancyrochitina ramosaspina* biozone was defined by Soufiane and Achab (2000) from the informal member 4 of the Gun River Formation (formalized as the Macgilvray Member by Copper et al., 2012) on Anticosti. Initially, the authors interpreted this biozone and assemblage as indicating a Rhuddanian age for the top of the Gun River Formation, but that has since been revised and reinterpreted as Aeronian (e.g., Copper and Jin, 2015). Following the original definition of the biozone and using the new data obtained at Jumpers Cliff, we extend this biozone up to the top of the Ferrum Member of the Jupiter Formation. The index species is absent from the lowest sample at Jumpers, but given its unambiguous records within underlaying strata, we suggest that the biozone starts at (and extends below) the base of the section in Fig. 8.

Soufiane and Achab (2000) mentioned the occurrence of *Euconochitina electa* and *Conochitina gunriveris* in this biozone, both found in the Ferrum Member of the Jupiter Formation in the Jumpers Cliff section. Additionally, the authors identified *Conochitina* cf. *proboscifera* in member 4 of the Gun River Formation. Based on picture 18 of plate III of Soufiane and Achab (2000), the described species is

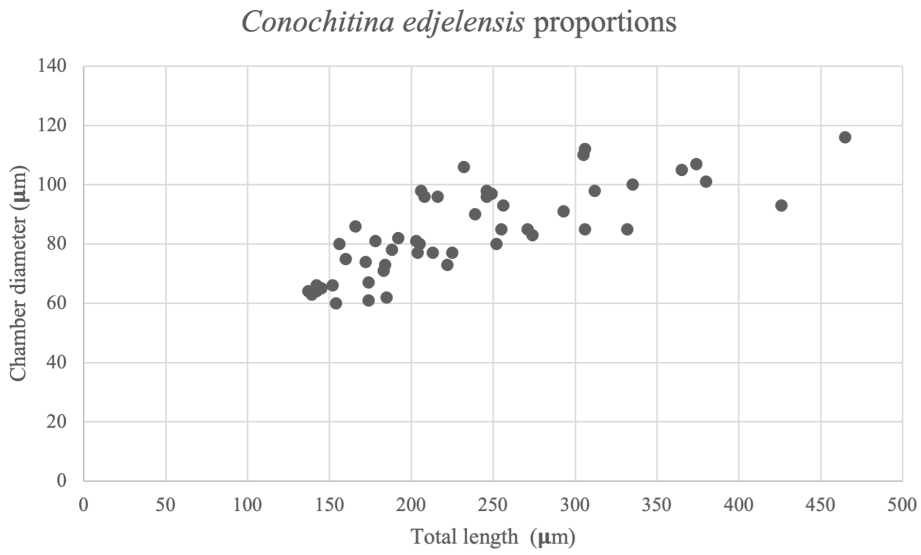

Figure 7. Size distribution within the *Conochitina edjelensis–Conochitina elongata* group (Taugourdeau, 1963). The total length of the specimens presents a considerably wider range – especially well-distributed in specimens smaller than 350 µm – than the chamber diameter.

actually *Conochitina praeproboscifera*. Achab (1981) also mentioned the occurrence of *Conochitina proboscifera* and *Conochitina* cf. *proboscifera* in the Jupiter Formation, and, based on figs. 1–3 of Plate IV and 15–17 of Plate V of the same paper, the taxa are reinterpreted to be *Conochitina praeproboscifera*.

In member 4 of the Gun River Formation, Soufiane and Achab (2000) reported *Bursachitina basiconcava* and an unidentified species of *Plectochitina*, both not found in the Ferrum Member of the Jupiter Formation in Jumpers Cliff.

In the Jumpers Cliff section, in addition to *Euconochitina electa*, *Conochitina gunriveris*, and *Conochitina praeproboscifera*, the *Ancyrochitina ramosaspina* biozone is marked by the presence of the *Conochitina edjelensis–elongata* group, *Conochitina malleus*, *Angochitina* sp. A, *Angochitina* sp. B, *Cyathochitina campanulaeformis*, and *Cyathochitina caputoi*. *Conochitina leptosoma* was locally identified in this biozone.

As to the wider correlation of this biozone, *Ancyrochitina ramosaspina* has been reported in the Baltic Basin in the assemblage of the *Spinachitina maennili* global biozone (Nestor, 2012) as well as together with *Conochitina alargada* (Loydell et al., 2010). It occurs straddling the base of the Aeronian (De Weirdt et al., 2020; Melchin et al., 2023) in a recently proposed replacement GSSP for the base of the Aeronian in Wales (UK). In Iran, *Ancyrochitina ramosaspina* has its LO below the LO of *Conochitina alargada* and defines a local biozone in the absence of *Spinachitina maennili* (Ghavidel-Syooki and Vecoli, 2007). Nonetheless, the Richardson Member is well-recognized as an upper Aeronian unit (e.g., Riva and Petryk, 1981; Copper and Jin, 2015; Braun et al., 2021) and the Ferrum Member is situated stratigraphically above it. Thus, it is reasonable to interpret the *Ancyrochitina ramosaspina* local biozone in the Ferrum Member as equivalent to the *Conochitina alargada* global biozone, below the LO of *Eisenackitina dolioliformis*, and typically Aeronian (i.e., *Ancyrochitina ramosaspina* and *Conochitina malleus*) or even older species (i.e., *Euconochitina electa*) as characterizing this biozone.

4.1.2 *Eisenackitina dolioliformis* biozone

Eisenackitina dolioliformis is the index species of the eponymous global biozone (Verniers et al., 1995). It has its LO in the Jumpers Cliff section in the Pavillon Member of the Jupiter Formation and ranges up to the highest productive sample of this study in the Chicotte Formation (Fig. 8). This biozone can be divided into two assemblages based on a faunal turnover that coincides with the limit between the Pavillon Member and the Chicotte Formation lithostratigraphical units.

The initial assemblage of the *Eisenackitina dolioliformis* biozone in the Pavillon Member of the Jupiter Formation has *Conochitina emmastensis*, which is characteristic of the *Eisenackitina dolioliformis* global biozone (Verniers et al., 1995; Nestor, 2012). Nestor (2012) also reports that *Conochitina leptosoma* and *Calpichitina densa* commonly co-occur with *E. dolioliformis*, and both of these taxa are indeed reported in the lower part of this biozone on Anticosti.

Spinachitina glooscapi sp. nov. is present in the pre-$\delta^{13}C$ portion of the *Eisenackitina dolioliformis* biozone, and *Angochitina* sp. A occurs only in the basalmost sample (JM-07) analyzed of the Pavillon Member. The *Conochitina edjelensis–elongata* group, *Conochitina gunriveris*, *Conochitina malleus*, *Conochitina praeproboscifera*, *Cy-*

athochitina campanulaeformis, and *Cyathochitina caputoi* continue to appear from the underlying biozone upwards.

In the middle of the Jumpers Cliff section, within the *Eisenackitina dolioliformis* biozone, between samples JM-12, JM-13, and JM-14, three species have their highest (local) occurrences (HOs): *Calpichitina densa*, *Spinachitina glooscapi*, and *Cyathochitina caputoi*.

An uppermost, discrete assemblage within the *Eisenackitina dolioliformis* biozone is limited to the single productive sample in the Chicotte Formation (Fig. 8). Diversity decreases considerably towards the top of the section, as most species disappear, leaving only *Conochitina gunriveris* and *Conochitina malleus* and two newly described species to characterize this younger assemblage, i.e., *Conochitina asselinae* sp. nov. and *Ancyrochitina wilsonae* sp. nov.

4.2 Relative ages of the upper Jupiter and lower Chicotte formations

Considering the lack of graptolites in the Ferrum Member (Riva and Petryk, 1981), the long range of the *D. staurognathoides* conodont biozone ranging from the mid-Aeronian to the end of Te1 (Zhang and Barnes, 2002; Munnecke and Männik, 2009), and the inconclusive character in terms of age assignment of the *Stricklandia planirostrata* brachiopod assemblage zone (Jin and Copper, 2000), the Telychian age assigned to the Ferrum Member of the Jupiter Formation should be considered interpretative as none of the factors considered exclude the possibility of the unit still being of late Aeronian age. The chitinozoan biostratigraphic data produced in this study, however, suggest the presence of an Aeronian assemblage in the Ferrum Member. *Ancyrochitina ramosaspina* is described in the *Coronograptus cyphus* and *Demirastrites triangulatus* graptolite biozones in the Baltic Basin (Nestor, 1994; Loydell et al., 2010). *Euconochitina electa* has its FAD and defines a global biozone in the Rhuddanian (Verniers et al., 1995). And *Conochitina malleus* typically occurs in the Baltic Basin in the global *Conochitina alargada* biozone (Loydell et al., 2010; Nestor, 2012). Therefore, the presence of the classically Rhuddanian to Aeronian *Euconochitina electa* and *Ancyrochitina ramosaspina*, as well as the occurrence of the Aeronian *Conochitina malleus*, the *Ancyrochitina ramosaspina* local biozone in the Ferrum Member of the Jupiter Formation of Anticosti Island has elements that link it to the Aeronian elsewhere and is interpreted to be late Aeronian in age. Further chitinozoan studies in the units between member 4 of the Gun River Formation and the Ferrum Member are ongoing (Jonckheere, unpublished data).

The *Eisenackitina dolioliformis* biozone has its base in the Pavillon Member and continues in the Chicotte Formation. The global chitinozoan biozonation of Verniers et al. (1995) puts the FAD of *dolioliformis* in the top of the Aeronian based on data from the western Baltic Basin (Umnova 1976). This relative age relies on the base of the Rumba Formation being Aeronian – an ongoing discussion (referred to in the Introduction). In the Llandovery area of the Welsh Basin, Davies et al. (2013) reported *Eisenackitina dolioliformis* in the upper Aeronian *convolutus* graptolite zone. Vandenbroucke et al. (2003) reported *Eisenackitina dolioliformis* in the Wood Burn Formation of the Girvan area (Scotland), where graptolites from the same level at a nearby locality belong to the upper Aeronian *sedgwickii* graptolite biozone. However, having studied these two UK assemblages as well as the one we describe here from Anticosti, we suggest that while the Welsh and Scottish taxa are seemingly conspecific, they are morphologically somewhat different from the specimens found in Anticosti and may not be conspecific with the latter. These considerations mainly reflect the ornamentation of the taxa – species of the genus *Eisenackitina* are characterized by a randomly distributed spiny ornamentation (Paris et al., 1999). Despite some small variability between the Anticosti specimens of *Eisenackitina dolioliformis* and those from the Baltic Basin (e.g., Nestor, 1994), both certainly present the same species and have spines covering their vesicles. The specimens shown in Vandenbroucke et al. (2003) and Davies et al. (2013) appear to have a similar vesicle shape to *E. dolioliformis*, as well as the typical thick walls, but there are no spines covering the vesicles. Furthermore, some authors (e.g., Mullins and Loydell, 2002, in the Welsh Basin; Loydell et al., 2010, in Latvia; Nestor, 2012, review and data compilation in the Baltic Basin; unpublished compiled data from Jacques Verniers, personal communication, 2023) mark the base of the *Eisenackitina dolioliformis* biozone in the Telychian – which, in the case of the eastern Baltic Basin, is just above a gap in the stratigraphy (see Sect. 4.3 and both Loydel et al., 2010, and Nestor, 2012). Consequently, this does not, in all likelihood, represent the global FAD of the species. In summary, while there seems to be a tendency in the more recent literature to restrict the *Eisenackitina dolioliformis* biozone to the Telychian, there also seem to be reports of the index species from the upper Aeronian. The latter Aeronian findings may not represent exactly the same taxon as the index species, so some uncertainty remains with regards to the exact age of the base of the *Eisenackitina dolioliformis* biozone. Here, given that the brachiopod and graptolite biozonations suggest a Telychian age for the unit, and considering that the Anticosti specimens of *Eisenackitina dolioliformis* more strongly resemble those of the Baltic Telychian than those of the UK Aeronian, it is reasonable to suggest that the presence of the *Eisenackitina dolioliformis* biozone likely indicates a Telychian age for the Pavillon Member on Anticosti Island. Nevertheless, solely based on chitinozoans, a latest Aeronian age for this member cannot be excluded, amongst others, because it is unclear what exactly the FAD of the "Baltic morphotypes" is, given the incomplete nature of those sections.

A further word of caution is warranted, as the coinciding LOs of various species (*Eisenackitina dolioliformis* and *Conochitina emmastensis*) and their coincidence with the

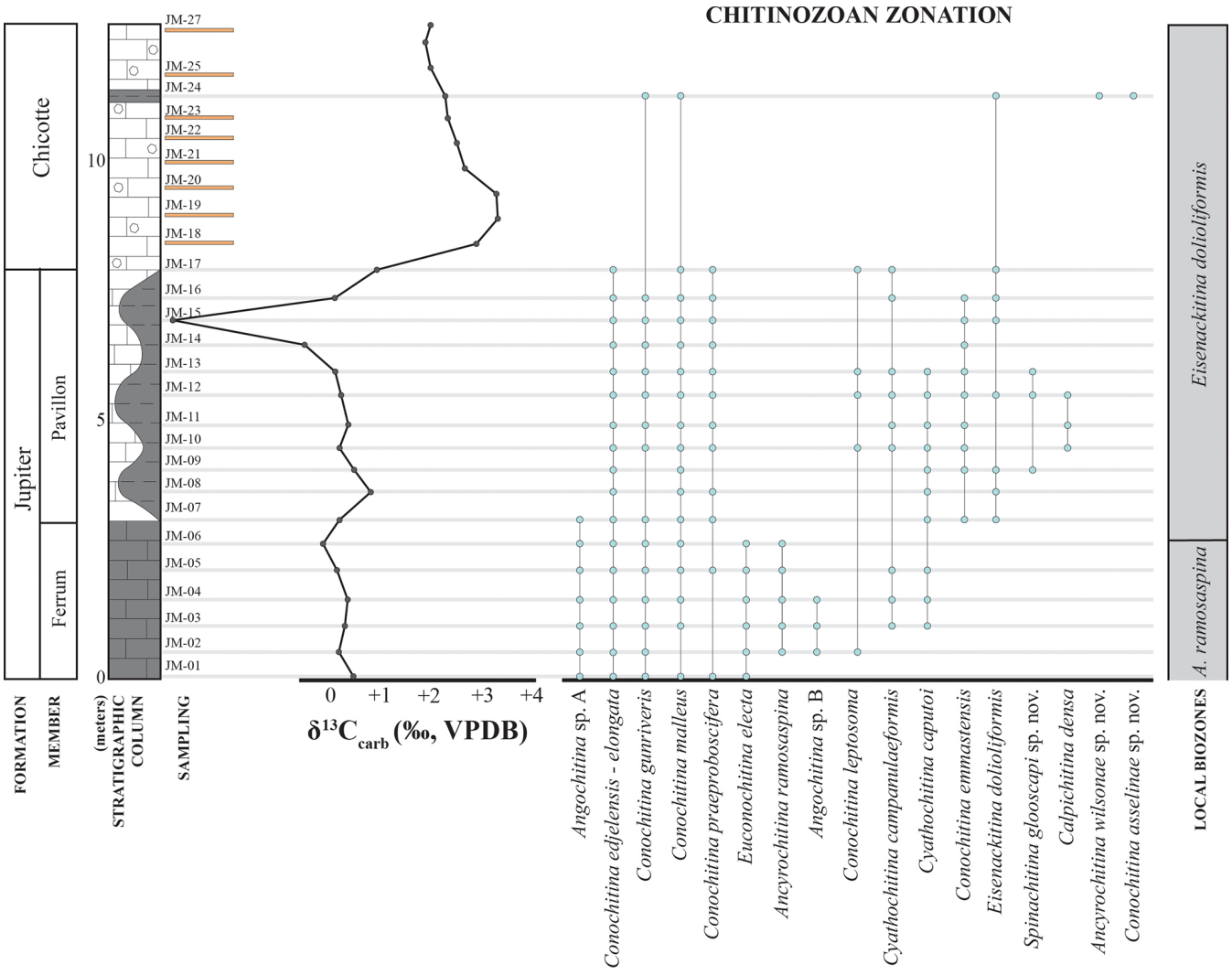

Figure 8. Chitinozoan ranges of Jumpers Cliff relative to lithology and $\delta^{13}C_{carb}$ records (modified from Braun et al., 2021). Yellow bars represent barren samples.

lithostratigraphical limit between the Ferrum and Pavillon members suggest that there are other controls on their stratigraphic ranges than mere temporal constrains. However, given the similarity of the sample facies between the two members and the typical Aeronian assemblages in the lower member, we do not think this influences the suggested age assignments of the units.

The Braun et al. (2021) chemostratigraphic data also place the peak of the $\delta^{13}C$ excursion relative to the Valgu event, globally reported at Te2 (Cramer et al., 2011), in the Chicotte Formation. $\delta^{13}C$ values are near 0 ‰ throughout the Ferrum Member and approach +1 ‰ at the bottom of the Pavillon Member for sample JM-08 (note that this is a sample of considerably low yield and diversity), probably marking initial disturbances to the carbon cycle and the beginning of the event. Towards the top of the Pavillon Member, for sample JM-15, there is an abrupt negative peak of −3 ‰, after which $\delta^{13}C$ values start to increase, building up to the main positive peak at the Chicotte Formation.

The proposed placement of the Ferrum Member of the Jupiter Formation of Anticosti Island in the upper Aeronian and the Pavillon Member of the Jupiter Formation (most likely) and the Chicotte Formation (certainly) in the lower Telychian, with compiled global and local biozones, is presented in Fig. 9.

4.3 Upper Aeronian–lower Telychian disconformities

This study makes a case for significant preservation of upper Aeronian strata above the late Aeronian event on Anticosti Island. Whereas in most localities the Aeronian–Telychian boundary is placed immediately above the late Aeronian $\delta^{13}C$ positive excursion, on Anticosti, where the positive excursion is reported in the Richardson Member

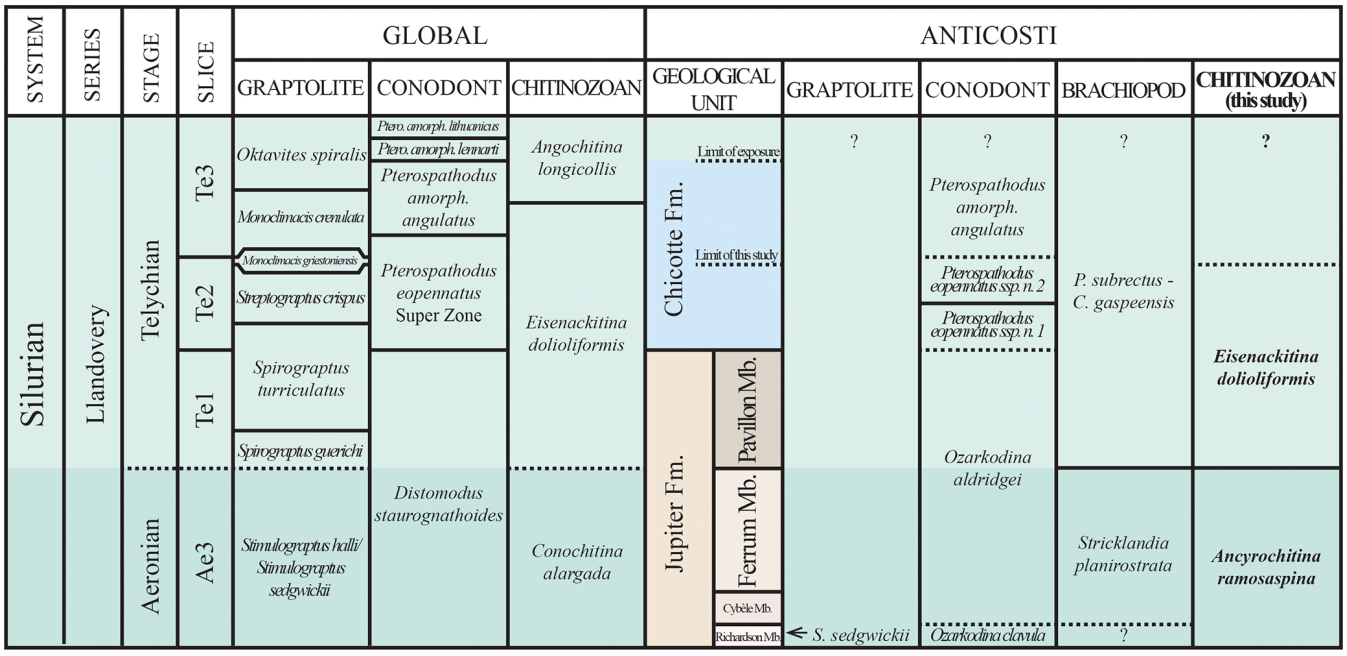

Figure 9. Upper Aeronian and lower Telychian units of Anticosti Island plotted with their local biozones (conodonts, Zhang and Barnes, 2002, and Munnecke and Männik, 2009; brachiopods, Jin and Copper, 2000; chitinozoans, this study) compared to the chronostratigraphy and "global" zones (after Melchin et al., 2020; chitinozoans, after Nestor, 2012). This diagram is illustrative only and not to temporal or lithostratigraphical scale.

(Braun et al., 2021), chitinozoan biostratigraphic data suggest that the strata comprising the Cybèle and Ferrum members still precede the Telychian, and the boundary is proposed to be between the Ferrum and the Pavillon members. Consequently, the record of lower Telychian strata appears to be more concise than previously thought, while still being well-preserved in comparison to other localities (Fig. 10). The Jupiter–Chicotte formational boundary represents a transgressive ravinement surface or a discontinuity surface as evidenced by an abrupt change from inner-ramp to mid-ramp packstones and grainstones with shale interbeds to more distal mid-ramp encrinites. Abrupt changes in $\delta^{13}C$ values in Braun et al. (2021), from less than +1 ‰ to +2.8 ‰, and the chitinozoan faunal turnover from the Pavillon Member to the Chicotte Formation support this interpretation.

Within the Pavillon Member, however, isotopic values published in Braun et al. (2021) define a negative shift from 0 ‰ to −0.5 ‰, jumping to −3 ‰ and then back to 0 ‰. At the onset of this negative shift, *Spinachitina glooscapi* and *Calpichitina densa* disappear from the *Eisenackitina dolioliformis* biozone. This could also represent an additional disconformity early in the Telychian, preceding the Valgu event on Anticosti Island.

Globally, gaps in sedimentation in the upper Aeronian and lower Telychian are also reported in the Baltic Basin (Munnecke and Männik, 2009; Nestor, 2012), as well as in the Michigan and Appalachian basins (McLaughlin et al., 2019). When comparing the lower Telychian strata of Anticosti Island and the Baltic Basin (Fig. 10), Anticosti displays a more comprehensive and expanded geological record of the Aeronian–Telychian boundary interval through the Valgu event.

5 Conclusions

A chitinozoan biostratigraphic study of the Jumpers Cliff section on Anticosti Island provides a refinement to the relative age of the boundary interval between the Jupiter and the Chicotte formations. A total of 18 productive samples were studied, with the highest chitinozoan diversity in the Pavillon Member (onset of the Valgu event) and lowest in the Chicotte Formation (peak of the positive $\delta^{13}C$ excursion of the Valgu event).

The Ferrum Member of the Jupiter Formation can be correlated with the global *Conochitina alargada* biozone (Verniers et al., 1995), given that it is locally attributed to the *Ancyrochitina ramosaspina* biozone (Soufiane and Achab, 2000). The *Ancyrochitina ramosaspina* biozone at Anticosti Island is thicker than previously reported (Soufiane and Achab, 2000), intersecting the global *sedgwickii* graptolite biozone in the Ae3 stage slice of the Aeronian stage and below the *Eisenackitina dolioliformis* biozone.

The Pavillon Member of the Jupiter Formation and the base of the Chicotte Formation are placed in the global *Eisenackitina dolioliformis* biozone. Given that the Anticosti specimens of *Eisenackitina dolioliformis* more strongly re-

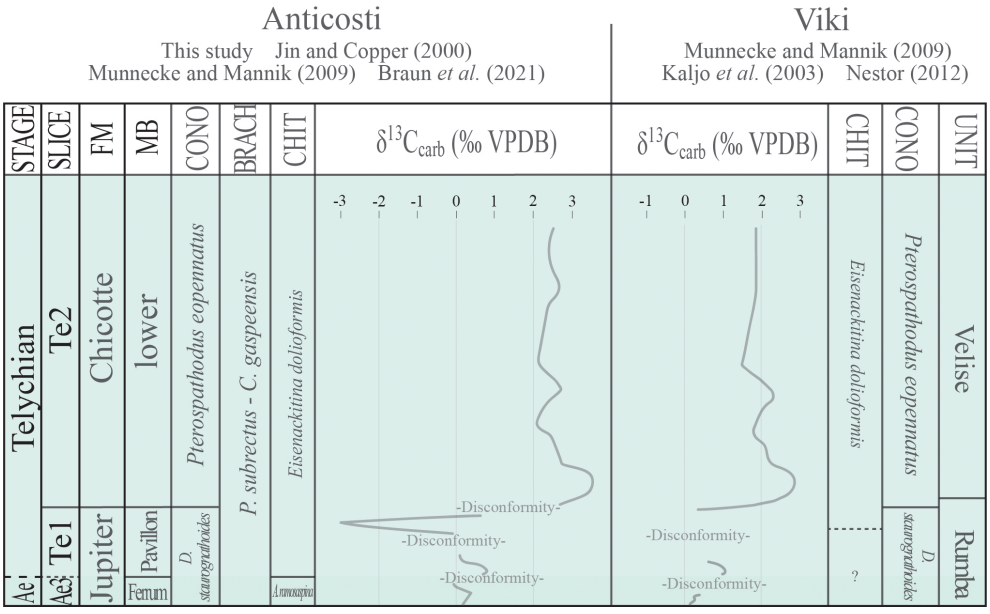

Figure 10. FM: formation; MB: member; CONO: conodonts; BRACH: brachiopods; CHIT: chitinozoans; Ae: Aeronian. Tentative chronostratigraphic correlation of the early Telychian units of Jumpers Cliff, Anticosti Island, and the Viki Core (Estonia) with chemostratigraphic data (Kaljo et al., 2003; Braun et al., 2021) as well as the conodont (Munnecke and Männik, 2009), brachiopod (only for Anticosti, Jin and Copper, 2000), and chitinozoan (this study and Nestor, 2012) biozones plotted.

semble those of the Baltic Telychian than those of the UK Aeronian, chitinozoans suggest a Telychian age for the Pavillon Member.

The chitinozoan data, coupled with conodont, brachiopod, and $\delta^{13}C$ stratigraphic data, point to a remarkable preservation of upper Aeronian strata on Anticosti Island. Disconformities are present in the middle of the Pavillon Member and at the base of the Chicotte Formation, indicated by abrupt facies change and offsets in $\delta^{13}C$ values (original data of Braun et al., 2021). Seemingly contemporary hiatuses are also present in the Baltic region (Munnecke and Männik, 2009) and in the Michigan and Appalachian basins (McLaughlin et al., 2019).

This refined age model for the Aeronian to Telychian succession of Anticosti Island provides a solid baseline for future studies of the Llandovery biochemical events in the aftermath of the Late Ordovician mass extinction. Ultimately, understanding the continuity of the record in this interval will require geochronological efforts.

Data availability. The chitinozoan data we refer to make up the dataset included in the paper and provided in Table 2. The chemostratigraphic dataset was published by Braun et al. (2021).

Author contributions. Conceptualization: CK, PIM, TRAV, AD, PE. Funding acquisition: TRAV, AD. Data collection: CK. Data contribution: FJ. Systematic description discussions: TdB, CJPE, TRAV. Writing: CK, PIM, TRAV, AD.

Competing interests. The contact author has declared that none of the authors has any competing interests.

Disclaimer. Any use of trade, firm, or product names is for descriptive purposes only and does not imply endorsement by the US government.

Publisher's note: Copernicus Publications remains neutral with regard to jurisdictional claims made in the text, published maps, institutional affiliations, or any other geographical representation in this paper. While Copernicus Publications makes every effort to include appropriate place names, the final responsibility lies with the authors.

Acknowledgements. Scanning electron microscope (SEM) images were generated using research infrastructure funded through FWO grant I013118N. Carolina Klock and Thijs Vandenbroucke received support from the HFSP – Human Frontiers Science Program (grant RGP0066/2021) and the research incubator of the Société du Patrimoine Mondial Anticosti. Thijs Vandenbroucke, Patrick McLaughlin, and Poul Emsbo acknowledge funding by the Research Foundation–Flanders (research grant G038722N, Monsters of the Apocalypse). Thijs Vandenbroucke also acknowledges support from the King Baudouin Foundation (Professor T. Van Autenboer Fund). Tim De Backer was funded through a Bijzonder Onderzoeksfonds-Universiteit Gent (BOF-UGent) starting grant (BOF17/STA/013 to Vandenbroucke). Cristiana J. P. Esteves is supported by an FCT PhD grant (SFRH/BD/144840/2019). The authors acknowledge Jacques Verniers for help with species identification

and global occurrences, Matthew Braun for discussions on Anticosti Island chemostratigraphy and published data as well as assistance in the field, Alyssa Bancroft for suggestions on text and figures, and Pascale Daoust for assistance during fieldwork. The authors want to thank Sabine Van Cauwenberghe for the palynological lab preparations. Lastly, the authors are grateful to the reviewers, Sonia Camina and one anonymous reviewer, for the valuable remarks and comments.

Financial support. This research has been supported by the Human Frontier Science Program (grant no. RGP0066/2021), the Fonds Wetenschappelijk Onderzoek (grant no. I013118N; G038722N), BOF (BOF/17/STA/013), an FCT PhD grant (SFRH/BD/144840/2019), and the research incubator of the Société du Patrimoine Mondial Anticosti.

Review statement. This paper was edited by Luke Mander and reviewed by Sonia Clara Camina and one anonymous referee.

References

Achab, A.: Biostratigraphie par les chitinozoaires, de l'Ordovicien Supérieur–Silurian Inférieur de l'île d'Anticosti. Résultats préliminaires, in: Field Meeting Anticosti-Gaspé – Subcommission on Silurian Stratigraphy, Ordovician – Silurian Boundary Working Group, edited by: Lespérance, P. J., Université de Montréal, Québec, 2, 143–157, 1981.

Achab, A., Asselin, E., Desrochers, A., Riva, and J. F., and Farley, C.: Chitinozoan biostratigraphy of a new Upper Ordovician stratigraphic framework for Anticosti Island, Canada, Geol. Soc. Am. Bull., 123, 186–205, https://doi.org/10.1130/B30131.1, 2011.

Achab, A., Esther, A., Desrochers, A., and Riva, J.F.: The end-Ordovician chitinozoan zones of Anticosti Island, Québec: definition and stratigraphic position, Rev. Palaeobot. Palynol., 198, 92–109, https://doi.org/10.1016/j.revpalbo.2012.07.019, 2013.

Barnes, C. R.: Stratigraphy and palaeontology of the Ordovician-Silurian boundary interval, Anticosti Island, Quebec, Bull. Br. Mus. Nat. Hist. Geol., 43, 195–219, 1988.

Barnes, C. R., Petryk, A. A., and Bolton, T. E.: Anticosti Island, Québec, in: Field Meeting Anticosti-Gaspé – Subcommission on Silurian Stratigraphy, Ordovician – Silurian Boundary Working Group, edited by: Lespérance, P. J., Université de Montréal, Québec, 1, 3–24, 1981.

Bengtson, P.: Open nomenclature, Palaeontology, 31, 223–227, 1988.

Bordet, E., Malo, M., and Kirkwood, D.: A structural study of western Anticosti Island, St. Lawrence platform, Quebec: a fracture analysis that integrates surface and subsurface structural data, Bull. Can. Petrol. Geol., 58, 36–55, https://doi.org/10.2113/gscpgbull.58.1.36, 2010.

Braun, M. G., Daoust, P., and Desrochers, A.: A sequential record of the Llandovery $\delta^{13}C_{carb}$ excursions paired with time-specific facies: Anticosti Island, eastern Canada, Palaeogeogr. Palaeocl., 578, 110566, https://doi.org/10.1016/j.palaeo.2021.110566, 2021.

Calner, M.: Silurian global events – at the tipping point of climate change, in: Mass Extinction, edited by: Elewa, A. M. T., Springer-Verlag Berlin, Heidelberg, Berlin, 21–58, https://doi.org/10.1007/978-3-540-75916-4, 2008.

Canadian Museum of History: Origin stories – Glooscap: https://www.historymuseum.ca/cmc/exhibitions/aborig/fp/fpz2f21e.html, last access: 18 December 2023.

Caputo, M. V. and dos Santos, R. O. B.: Stratigraphy and ages of four Early Silurian through Late Devonian, Early and Middle Mississippian glaciation events in the Parnaíba Basin and adjacent areas, NE Brazil, Earth Sci. Rev., 207, 103002, https://doi.org/10.1016/j.earscirev.2019.103002, 2020.

Clayer, F. and Desrochers, A.: The stratigraphic imprint of a mid-Telychian (Llandovery, early Silurian) glaciation on far-field shallow-water carbonates, Anticosti Island, Eastern Canada, Estonian J. Earth Sci., 63, 207–213, https://doi.org/10.3176/earth.2014.20, 2014.

Cocks, L. R. M. and Worsley, D.: Late Llandovery and early Wenlock stratigraphy and ecology in the Oslo Region, Norway. Bull. Brit. Mus., Geol., 49, 31–46, https://doi.org/10.5962/p.313804, 1993.

Copper, P. and Long, D. G. F.: Stratigraphic revision of the Jupiter Formation, Anticosti Island, Canada; a major reference section above the Ordovician-Silurian Boundary, Newsl. Stratigr., 23, 11–36, 1990.

Copper, P. and Jin, J.: Early Silurian (Aeronian) East Point Coral Patch Reefs of Anticosti Island, Eastern Canada: first Reef Recovery from the Ordovician/Silurian Mass Extinction in Eastern Laurentia, Geosciences, 2, 64–89, https://doi.org/10.3390/geosciences2020064, 2012.

Copper, P. and Jin, J.: The revised Lower Silurian (Rhuddanian) Becscie Formation, Anticosti Island, eastern Canada records the tropical marine faunal recovery from the end-Ordovician Mass Extinction, Newsl. Stratigr. 47, 61–83, https://doi.org/10.1127/0078-0421/2014/0040, 2014.

Copper, P. and Jin, J.S.: Tracking the early Silurian post-extinction faunal recovery in the Jupiter Formation of Anticosti Island, eastern Canada: A stratigraphic revision, Newsl. Stratigr., 48, 221–240, https://doi.org/10.1127/nos/2015/0061, 2015.

Copper, P., Long, D. G. F., and Jin, J.: The Early Silurian Gun River Formation of Anticosti Island, eastern Canada: a key section for the mid-Llandovery of North America, Newsl. Stratigr., 45, 263–280, https://doi.org/10.1127/0078-0421/2012/0024, 2012.

Cramer, B. D., Brett, C. E., Melchin, M. J., Männik, P., Kleffner, M. A., McLaughlin, P. I., Loydell, D. K., Munnecke, A., Jeppsson, L., Corradini, C., Brunton, F. R., and Saltzman, M. R.: Revised chronostratigraphic correlation of the Silurian System of North America with global and regional chronostratigraphic units and $\delta^{13}C_{carb}$ chemostratigraphy, Lethaia, 44, 185–202, https://doi.org/10.1111/j.1502-3931.2010.00234.x, 2011.

Cramer, F. H.: Microplankton from three Palaeozoic formations in the province of Leon, NW Spain, Leidse Geol. Meded., 30, 253–261, 1964.

Cramer, F. H.: Chitinozoans of a composite section of Upper Llandoverian to basal Lower Gedinnian sediments in northern Leon, Spain, Bull. Soc. Belge Géol. Paléont. Hydrol., 75, 69–129, 1967.

Da Costa, N. M.: Quitinozoários Silurianos do Igarapé da Rainha, Estado do Pará. Divisão de Geologia e Mineralogia, Departamento Nacional de Produção Minera, Boletim, 255, 1–101, 1971.

Davies, J., Waters, R., Molyneux, S., Williams, M., Zalasiewicz, J., Vandenbroucke, T., and Verniers, J.: A revised sedimentary and biostratigraphical architecture for the Type Llandovery area, Central Wales, Geol. Mag., 150, 300–332, https://doi.org/10.1017/S0016756812000337, 2013.

Desrochers, A.: Rocky shoreline deposits in the Lower Silurian (Upper Llandovery, Telychian) Chicotte Formation, Anticosti Island, Québec, Can. J. Earth Sci., 43, 1205–1214, https://doi.org/10.1139/e06-054, 2006.

Desrochers, A., Farley, C., Achab, A., Asselin, A., and Riva, J. F.: A far-field record of the end Ordovician glaciation: the Ellis Bay Formation, Anticosti Island, Eastern Canada, Palaeogeogr. Palaeocl., 296, 248–263, https://doi.org/10.1016/j.palaeo.2010.02.017, 2010.

Desrochers, A., Jin, J., and Dewing, K.: The Ordovician System of Canada: an extensive stratigraphic record of Laurentian shallow water platforms and deep marine basins, Geol. Soc. Lond., 533, 65–92, 2023.

De Weirdt, J., Vandenbroucke, T. R. A., Cocq, J., Russell, C., Davies, J. R., Melchin, M., and Zalasiewicz, J.: Chitinozoan biostratigraphy of the Rheidol Gorge Section, Central Wales, UK: a GSSP replacement candidate for the Rhuddanian–Aeronian boundary, Pap. Palaeontol., 6, 173–192, https://doi.org/10.1002/spp2.1260 2020.

Eisenack, A.: Neue Mikrofossilien des baltischen Silurs, I, PalZ., 13, 74–118, 1931.

Eisenack, A.: Chitinozoen, Hystrichosphaeren und andere Mikrofossilien aus dem Beyrichia-Kalk, Senckenb, Lethaea, 36, 157–188, 1955.

Eisenack, A.: Neotypen baltischer Silur: chitinozoen und neue arten, Neues Jahrbuch für Geologie und Paläontologie, Abhandlungen, 108, 1–20, 1959.

Eisenack, A.: Neotypen baltischer Silur-Chitinozoen und neue Arten, Neues Jahrbuch für Geologie und Paläontologie, Abhandlungen, 114, 291–316, 1962.

Eisenack, A.: Beitrage zur Chitinozoen-Forschun, Palaeontogr. Abt. A, 131, 137–198, 1972.

Ghavidel-Syooki, M. and Vecoli, M.: Latest Ordovician–early Silurian chitinozoans from the eastern Alborz Mountain Range, Kopet–Dagh region, northeastern Iran: biostratigraphy and palaeobiogeography, Rev. Palaeobot. Palynol., 145, 173–192, https://doi.org/10.1016/j.revpalbo.2006.10.003, 2007.

Grahn, Y., Pereira, E., and Bergamaschi, S.: Silurian and Lower Devonian Chitinozoan Biostratigraphy of the Paranaì Basin in Brazil and Paraguay, Palynology, 24, 147–176, https://doi.org/10.1080/01916122.2000.9989542, 2000.

Grahn, Y., Melo, J. H. G., and Steemans, P.: Contribution to the integrated chitinozoan and miospore biostratigraphy of the Serra Grande Group (Silurian – Lower Devonian) in the Parnaìba Basin, northeast Brazil, Rev. Esp. Micropaleontol., 37, 183–204, 2005.

Gouldey, J. C., Saltzman, M. R., Young, S. A., and Kaljo, D.: Strontium and carbon isotope stratigraphy of the Llandovery (Early Silurian): implications for tectonics and weathering, Palaeogeogr. Palaeocl., 296, 264–275, https://doi.org/10.1016/j.palaeo.2010.05.035, 2010.

Jeppsson, L.: Silurian events: the theory and the conodonts, Prec. Estonian Acad. Sci., 42, 13–27, 1993.

Jia-Yu, R. and Johnson, M. E.: A stepped karst unconformity as an Early Silurian rocky shoreline in Guizhou Province (South China), Palaeogeogr. Palaeocl., 121, 115–129, https://doi.org/10.1016/0031-0182(95)00082-8, 1996.

Jin, J.: The early Silurian pentamerid brachiopod Costistricklandia canadensis (Billings, 1859) and its biostratigraphic and paleobiogeographic significance, J. Paleontol., 76, 638–647, 2002.

Jin, J. and Copper, P.: Late Ordovician and Early Silurian pentamerid brachiopods of Anticosti Island, Québec, Canada, Palaeontogr. Can., 18, 1–140, https://doi.org/10.1017/S0022336000030973, 2000.

Kaljo, D. and Martma, T.: Carbon isotopic composition of Llandovery rocks (East Baltic Silurian) with environmental interpretation, Proc. Estonian Acad. Sci. Geol., 49, 267–283, https://doi.org/10.3176/geol.2000.4.02, 2000.

Kaljo, D., Martma, T., Männik, P., and Viira, V.: Implications of Gondwana glaciations in the Baltic late Ordovician and Silurian and a carbon isotopic test of environmental cyclicity, Bull. Soc. Géol. Fr., 174, 59–66, https://doi.org/10.2113/174.1.59, 2003.

Laufeld, S.: Silurian Chitinozoa from Gotland, Fossils and Strata, 5, 1–130, 1974.

Long, D. G. F.: Tempestite frequency curves: a key to Late Ordovician and Early Silurian subsidence, sea-level change, and orbital forcing in the Anticosti foreland basin, Québec, Canada, Can. J. Earth Sci., 44, 413–431, https://doi.org/10.1139/e06-099, 2007.

Loydell, D. K., Nestor, V., and Männik, P.: Integrated biostratigraphy of the lower Silurian of the Kolka-54 core, Latvia, Geol. Mag., 147, 253–280, https://doi.org/10.1017/S0016756809990574, 2010.

McLaughlin, P. I., Emsbo, P., Desrochers, A., Bancroft, A., Brett, C. E., Riva, J. F., Premo, W., Neymark, L., Achab, A., Asselin, E., and Emmons, M.: Refining 2 km of Ordovician chronostratigraphy beneath Anticosti Island utilizing integrated chemostratigraphy, Can. J. Earth Sci., 53, 1–10, https://doi.org/10.1139/cjes-2015-0242, 2016.

McLaughlin, P. I., Emsbo, P., Brett, C. E., Bancroft, A. M., Desrochers, A., and Vandenbroucke, T. R. A.: The rise of pinnacle reefs: A step change in marine evolution triggered by perturbation of the global carbon cycle, Earth Planet. Sc. Lett., 515, 13–25, https://doi.org/10.1016/j.epsl.2019.02.039, 2019.

Melchin, M. J., Sadler, P. M., and Cramer, B. D.: The Silurian Period, in: Geologic Time Scale 2020, Vol. 2, edited by: Gradstein, F. M., Ogg, J. G., Schmitz, M. D., and Ogg, G. M., Elsevier, Amsterdam, 695–732, https://doi.org/10.1016/C2020-1-02369-3, 2020.

Melchin, M. J., Davies, J. R., Boom, A., De Weirdt, J., McIntyre, A. J., Russell, C., Vandenbroucke, T. R. A., and Zalasiewicz, J. A.: Integrated stratigraphical study of the Rhuddanian-Aeronian (Llandovery, Silurian) boundary succession in the Rheidol Gorge, Wales: A proposed Global Stratotype Section and Point for the base of the Aeronian Stage, Lethaia, 56, 1–23, https://doi.org/10.18261/let.56.1.8, 2023.

Merdith, A. S., Williams, S. E., Collins, A. S., Tetley, M. G., Mulder, J. A., Blades, M. L., Young, A., Armistead, S. E., Cannon, J., Zahirovic, S., and Müller, R. D.: Extending full-plate tectonic models into deep time: Linking the Neopro-

terozoic and the Phanerozoic, Earth Sci. Rev., 214, 103477, https://doi.org/10.1016/j.earscirev.2020.103477, 2021.

Mullins, G. L. and Loydell, D. K.: Integrated lower Silurian chitinozoan and graptolite biostratigraphy of Buttington Brick Pit, Wales. Geol. Mag., 139, 89–96, https://doi.org/10.1017/S001675680100591X, 2002.

Munnecke, A. and Männik, P.: New biostratigraphic and chemostratigraphic data from the Chicotte Formation (Llandovery, Anticosti Island, Laurentia) compared with the Viki core (Estonia, Baltica), Estonian J. Earth Sci., 58, 159–169, https://doi.org/10.3176/earth.2009.3.01, 2009.

Munnecke, A., Calner, M., Harper, D. A. T., and Servais, T.: Ordovician and Silurian Sea- water chemistry, sea level, and climate: a synopsis, Palaeogeogr. Palaeocl., 296, 389–413, https://doi.org/10.1016/j.palaeo.2010.08.001, 2010.

Nestor, V.: New Chitinozoan species from the Lower Llandoverian of Estonia, Eesti NSV Teaduste Akadeemia Toimetised, 29, 98–107, 1980a (in Russian with English translation).

Nestor, V.: Middle Llandoverian Chitinozoans from Estonia, Eesti NSV Teaduste Akadeemia Toimetised, 29, 136–42, 1980b (in Russian with English translation).

Nestor, V.: New Wenlockian species of Conochitina from Estonia, P. Est. Acad. Sci., 31, 105–110, 1982.

Nestor, V.: Silurian chitinozoans, in: Field Meeting, Estonia – An Excursion Guidebook, edited by: Kaljo, D., and Nestor, H., Institute of Geology, P. Est. Acad. Sci., Tallinn, 80–83, 1990.

Nestor, V.: Early Silurian Chitinozoans of Estonia and North Latvia, Academia, 4, 1–163, 1994.

Nestor, V.: A summary and revision of the East Baltic Silurian chitinozoan biozonation, Estonian J. Earth Sci., 61, 242–260, https://doi.org/10.3176/earth.2012.4.05, 2012.

Paris, F.: Les chitinozoaires dans le Paléozoïque du sud-ouest de l'Europe (cadre géologique-étude systématique-biostratigraphie), Bull. Soc. Géol. Minéral. Bretagne, 26, 1–496, 1981.

Paris, F. and A1-Hajri, S.: New chitinozoan species from Llandovery subsurface strata of Saudi Arabia, Rev. Micropaleontol., 38, 311–328, 1995.

Paris, F., Grahn, Y., Nestor, V., and Lakova, I.: A revised chitinozoan classification, J. Paleontol., 73, 549–70, https://doi.org/10.1017/S0022336000032388, 1999.

Pinet, N., Keating, P., Lavoie, L., Dietrich, J., Duchesne, M., and Brake, V.: Revisiting the Appalachian structural front and offshore Anticosti Basin (northern Gulf of St. Lawrence, Canada) by integrating old and new geophysical datasets, Mar. Petrol. Geol., 32, 50–62, https://doi.org/10.1016/j.marpetgeo.2011.12.004, 2012.

Pinet, N., Brake, V., and Lavoie, D.: Geometry and regional significance of joint sets in the Ordovician-Silurian Anticosti Basin: New insights from fracture mapping, Geological Survey of Canada, Open File 7752, 26 pp., https://doi.org/10.4095/295982, 2015.

Riva, J. F. and Petryk, A. A.: Graptolites from the Upper Ordovician and Lower Silurian of Anticosti Island and the Position of the Ordovician-Silurian Boundary, in: Field Meeting Anticosti-Gaspé – Subcommission on Silurian Stratigraphy, Ordovician–Silurian Boundary Working Group, edited by: Lespérance, P. J., Université de Montréal, Québec, 143–157, 1981.

Sami, T. and Desrochers, A.: Episodic sedimentation on an Early Silurian, storm-dominated carbonate ramp, Becscie and Merrimack Formations, Anticosti Island, Canada, Sedimentology, 39, 355–381, https://doi.org/10.1111/j.1365-3091.1992.tb02122.x, 1992.

Schallreuter, R.: Neue Chitinozoen aus ordovizischen Geschieben und Bemerkungen zur Gattung Illichitina, Paläontol. Abh., 1, 392–405, 1963.

Soufiane, A. and Achab, A.: Chitinozoan zonation of the Late Ordovician and the Early Silurian of the island of Anticosti, Quèbec, Canada. Rev. Palaeobot. Palynol., 109, 85–111, https://doi.org/10.1016/S0034-6667(99)00044-5, 2000.

Sutherland, S. J. E.: Ludlow chitinozoans from the type area and adjacent regions, Palaeontogr. Soc. Monogr., 148, 1–104, https://doi.org/10.1080/25761900.2022.12131775, 1994.

Taugourdeau, P.: Étude de quelques espèces critiques de Chitinozoaires de la région d'Edjete et complements a la faune locale, Rev. Micropaleontol., 6, 130–44, 1963.

Taugourdeau, P.: Les Chitinozoaires, techniques d'études, morphologie et classification, Mém. Soc. Géol. Fr. Nouv., 45, 1–64, 1966.

Umnova, N. I.: Structural types of the prosome and operculum in the Chitinozoa and their association with genera and species, Paleontol. J., 4, 393–406, 1976.

Vandenbroucke T., Verniers, J., and Clarkson, E. N. K.: A chitinozoan biostratigraphy of the Upper Ordovician and the lower Silurian strata of the Girvan area, Midland Valley, Scotland, Trans. Roy. Soc. Edinb. Earth Sci., 93, 111–134, https://doi.org/10.1017/S0263593300000365, 2003.

Verniers, J., Nestor, V., Paris, F., Dufka, P., Sutherland, S., and Van Grootel, G.: A global Chitinozoa biozonation for the Silurian, Geol. Mag., 132, 651–666, https://doi.org/10.1017/S0016756800018896, 1995.

Walasek, N., Loydell, D. K., Frýda, J., Männik, P., and Loveridge, R. F.: Integrated graptolite-conodont biostratigraphy and organic carbon chemostratigraphy of the Llandovery of Kallholn quarry, Dalarna, Sweden, Palaeogeogr. Palaeocl., 508, 1–16, https://doi.org/10.1016/j.palaeo.2018.08.003, 2018.

Zhang, S. and Barnes, C.: A new Llandovery (Early Silurian) conodont biozonation and conodonts from the Becscie, Merrimack, and Gun River formations, Anticosti Island, Quebec, J. Paleontol., 76, 1–46, https://doi.org/10.1666/0022-3360(2002)76[1:ANLESC]2.0.CO;2, 2002.

Zimmt, J. B., Holland, S. M., Desrochers, A., Jones, D. S., and Finnegan, S.: A high-resolution sequence stratigraphic framework for the eastern Ellis Bay Formation, Canada: A record of Hirnantian sea-level change, GSA Bull., 136, 3825–3849, https://doi.org/10.1130/B37190.1, 2024.